Cell, Vol. 98, 377–386, August 6, 1999, Copyright ©1999 by Cell Press

Oligomeric Complexes Link Rab5 Effectors with NSF and Drive Membrane Fusion via Interactions between EEA1 and Syntaxin 13

Heidi M. McBride,*† Vladimir Rybin,*† Carol Murphy,‡ Angelika Giner,*† Rohan Teasdale,§ and Marino Zerial*†‖

*European Molecular Biology Laboratory
Meyerhofstrasse 1
69117 Heidelberg
Germany

†Max Planck Institute for Molecular Cell Biology and Genetics
Pfotenhauerstrasse
01307 Dresden
Germany

‡Laboratory of Biological Chemistry
Medical School
University of Ioannina
45110 Ioannina
Greece

§Monash Medical School
Department of Pathology and Immunology
Commercial Road
Prahran
Victoria 3181
Australia

Summary

SNAREs and Rab GTPases cooperate in vesicle transport through a mechanism yet poorly understood. We now demonstrate that the Rab5 effectors EEA1 and Rabaptin-5/Rabex-5 exist on the membrane in high molecular weight oligomers, which also contain NSF. Oligomeric assembly is modulated by the ATPase activity of NSF. Syntaxin 13, the t-SNARE required for endosome fusion, is transiently incorporated into the large oligomers via direct interactions with EEA1. This interaction is required to drive fusion, since both dominant-negative EEA1 and synthetic peptides encoding the FYVE Zn^{2+} finger hinder the interaction and block fusion. We propose a novel mechanism whereby oligomeric EEA1 and NSF mediate the local activation of syntaxin 13 upon membrane tethering and, by analogy with viral fusion proteins, coordinate the assembly of a fusion pore.

Introduction

Intracellular vesicle traffic from yeast to mammals has an absolute requirement for Rab GTPases (Novick and Zerial, 1997; Schimmoller et al., 1998). Rab proteins regulate membrane tethering and are also thought to be upstream modulators of the integral membrane SNARE proteins implicated in bilayer fusion (Lian et al., 1994; Søgaard et al., 1994; Lupashin and Waters, 1997). SNARE proteins are essential in all vesicle transport events to date and have been the focus of intense investigation, culminating most recently in the flurry of structural information on the stable syntaxin 1/Vamp2/SNAP25 ternary complex (Hanson et al., 1997; Hohl et al., 1998; Poirier et al., 1998; Sutton et al., 1998). Besides these important structural advances, the precise architectural arrangement of SNAREs in a fusion pore during lipid bilayer fusion remains an open question. This is an important consideration in light of recent studies demonstrating that although SNAREs may constitute the minimal machinery to mediate vesicle fusion in vitro (Weber et al., 1998), the low efficiency of this reaction in vitro strongly suggests that additional proteins are required for docking and fusion in vivo. Furthermore, the precise requirement for trans SNARE pairs remains controversial in light of recent data (Coorssen et al., 1998; Peters and Mayer, 1998; Ungermann et al., 1998). Therefore, although proteins of the SNARE machinery are clearly key players in intracellular traffic, they must act within a network of molecules, which together define transport specificity, facilitate vesicle docking, and ultimately drive bilayer fusion. It is likely that one of the requirements for these additional proteins may be to facilitate the regulated formation of macromolecular fusion pores.

One class of proteins known to participate within this network of interactions are the Rab GTPases and their effector molecules (Novick and Zerial, 1997; Gonzalez and Scheller, 1999). Recently, a large number of Rab effectors have been identified. This complexity may be required for the coordination of vesicle budding, motility, docking, and fusion (Novick and Zerial, 1997; Pfeffer, 1999). The direct evidence linking Rab GTPases and the proteins mediating vesicle docking is 2-fold. First, the Rab5 effector protein EEA1 has been recently been shown to function directly as a tethering protein in early endosome fusion (Christoforidis et al., 1999). Second, studies in budding yeast have demonstrated that Sec4p on secretory vesicles can directly interact with a component of the exocyst, thought to define the docking site at the tip of the yeast bud (Finger et al., 1998; Guo et al., 1999). Although tethering proteins like Uso1p/p115 (Nakamura et al., 1997; Cao et al., 1998), Sec35p (VanRheenen et al., 1998), and EEA1 (Christoforidis et al., 1999) have been identified, we do not know how Rab-dependent docking is molecularly coupled to the activation or assembly of the fusion machinery (Bean and Scheller, 1997). There are two possible requirements with respect to the regulation of SNARE function. First, given the broad distribution of SNAREs (von Mollard et al., 1997; Hay et al., 1998; Holthuis et al., 1998; Yang et al., 1999), there must be a defined docking site on the target membrane where these molecules are locally activated to ensure the specificity of the targeting event. Second, the activation of SNARE proteins, or priming by NSF and α-SNAP, must be regulated temporally and spatially. The effector protein EEA1 (Mu et al., 1995; Simonsen et al., 1998) was shown to be a core component of the docking and fusion machinery, since it alone could replace the requirement for cytosol in the early

‖To whom correspondence should be addressed (e-mail: zerial@embl-heidelberg.de).

endosome fusion assay (Christoforidis et al., 1999). The efficiency of this reaction suggested that EEA1 may have a mechanistic role in fusion as well as its role in tethering. In this study we have therefore searched for molecular links between the Rab machinery controlling early endosome tethering and SNARE-mediated fusion.

Results

Syntaxin 13 Functions in Early Endosome Fusion

In order to understand the molecular events mediating endosome fusion, it was first essential to identify the t-SNARE responsible for this transport event. We analyzed a panel of reagents in an in vitro homotypic early endosome fusion assay focusing on candidate t-SNAREs localized to endocytic structures. The soluble domains of recombinant syntaxins 3, 4 (Bennett et al., 1993), 7 (Advani et al., 1998; Wong et al., 1998), and 13 (Prekeris et al., 1998; Tang et al., 1998; Chao et al., 1999) and corresponding antibodies were tested in the fusion assay. The only syntaxin to demonstrate a specific, dose-dependent (data not shown), and inhibitory effect on endosome fusion was syntaxin 13 (Figure 1A). Endosome fusion was efficiently blocked by both recombinant syntaxin 13 at a concentration of 30 μM and by the corresponding antiserum (Figure 1A). The inhibition of the anti-syntaxin 13 antibody was specific, since it could be rescued by recombinant GST-tagged syntaxin 13 (20 μM), which, at this concentration, had only a modest inhibitory effect in comparison with the cleaved counterpart (Figure 1A). In contrast, both recombinant syntaxins 1, 2 (Bennett et al., 1993), and 6 (Bock et al., 1997; Klumperman et al., 1998) and corresponding antibodies had no effect (data not shown), further underscoring the specificity of syntaxin 13 in endosome fusion. This function is consistent with the localization of syntaxin 13 predominantly on early and tubular recycling endosomes (Prekeris et al., 1998; Tang et al., 1998).

Direct Interaction between EEA1 and Syntaxin 13

Having established that syntaxin 13 is the t-SNARE functioning in endosome fusion, we tested a direct interaction between the docking molecule EEA1 and syntaxin 13. We considered that such an interaction may be transient, rather than a stable complex at steady state, and therefore employed biosensor technology for analysis (Gournier et al., 1998). The advantage of this technique is that it allows the measurement of real-time association and dissociation of proteins on a sensor along with the estimation of protein affinities. We observed a specific interaction with syntaxin 13 to the carboxy-terminal region of EEA1(1257–1411)GST (Figure 1B). In contrast, no significant binding to the amino-terminal region of EEA1(1–209)GST was detected (data not shown). Of those recombinant syntaxins tested (up to 20 μM), syntaxins 3 and 7 did not demonstrate significant interactions with EEA1(1257–1411)GST (Figure 1B). Syntaxin 4 interacted weakly in the biosensor assay and since it had no effect in early endosome fusion, its significance is unclear. The concentration range required for the interaction with syntaxin 13 falls between 1.8 μM to 30 μM (Figure 1C). We estimated the apparent K_D of the carboxy-terminal interaction with syntaxin 13 to be ~18 μM as calculated from linear plots of the single phase association rates versus ligand concentrations. Interestingly, this K_D is comparable with that of syntaxin 1 and VAMP2 (4.7 μM) (Calakos et al., 1994). The rate of dissociation is very fast, 0.019 s^{-1}, which underscores the transient nature of the interaction. Considering that we have used bacterially expressed truncated proteins for this study (given the lack of full-length EEA1 in sufficient concentration and amount), it is possible that the affinity of native interactions on the membrane may be underestimated (see below). These experiments nevertheless

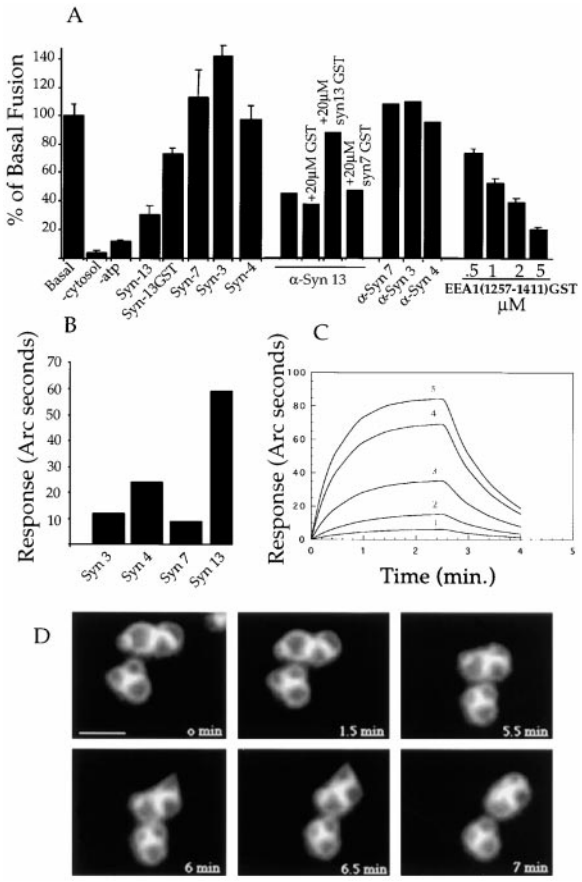

Figure 1. Syntaxin 13 Is Required for Endosome Fusion and Binds to EEA1

(A) Thirty micromolar recombinant syntaxins (lacking the transmembrane domains [ΔC]), 0.5 μl antibody serum or purified IgG (syntaxin 3 and 4), or increasing concentrations (μM) of recombinant EEA1(1257–1411)GST were added to standard fusion reaction as indicated. Inhibition by syntaxin 13 serum was rescued by the addition of 20 μM recombinant syntaxin 13GST, and not 20 μM syntaxin 7GST or 20 μM GST. Control reactions (minus cytosol or ATP) are indicated.

(B) Biosensor analysis demonstrates a direct interaction between EEA1 and syntaxin 13. EEA1(1257–1411)GST was immobilized on a biosensor chip before the addition of 20 μM either syntaxin 3ΔC, syntaxin 4ΔC, syntaxin 7ΔC, or syntaxin 13ΔC.

(C) Increasing concentrations of syntaxin 13ΔC were tested, and each sensogram is depicted: 1, 1.8 μM; 2, 3.75 μM; 3, 10 μM; 4, 18 μM; and 5, 29 μM. Background values for (B) and (C) (syntaxin binding to immobilized GST) were subtracted from each signal obtained with EEA1(1257–1411)GST.

(D) BHK cells were cotransfected with mycRab5Q79L and EEA1 (1257–1411)GFP and visualized by time-lapse video microscopy.

provide evidence for a specific interaction between EEA1 and syntaxin 13.

The Interaction between EEA1 and Syntaxin 13 Is Required for Endosome Fusion

Two lines of evidence suggest that the interaction between endogenous EEA1 and syntaxin 13 is necessary for fusion. First, recombinant EEA1(1257–1411)GST, which binds syntaxin 13, efficiently blocked the homotypic fusion with an IC50 of ~1.5 μM (Figure 1A) (Mills et al., 1998; Simonsen et al., 1998), suggesting that the EEA1 mutant interferes with the interaction between endogenous EEA1 and syntaxin 13. Interestingly, the value is lower than the observed K_D (18 μM) measured in the biosensor assay, arguing that the affinity of EEA1(1257–1411) for syntaxin 13 is higher in the presence of native proteins (see Discussion). The equivalent GFP fusion construct was also analyzed in living cells by video microscopy. In cells coexpressing EEA1(1257–1411)GFP and Rab5Q79L, this mutant had a unique property in that it did not just induce a kinetic block which delayed fusion temporarily, but arrested fusion over several minutes at the point of vesicle docking, as demonstrated by the movement of vesicles in clusters (Figure 1D). Second, since the inhibition of the C-terminal region of EEA1 may involve sequences other than binding syntaxin 13, we designed synthetic peptides to more selectively interfere with the EEA1/syntaxin 13 interaction. Figure 2A illustrates the domain structure within this region of EEA1. Five 20-amino-acid peptides corresponding to the IQ domain (amino acids 1349–1405), the Rab5-binding domain (1277–1411) (Simonsen et al., 1998), and the PI(3)P-binding Zn^{2+} FYVE finger domain (1351–1411) of EEA1 (Burd and Emr, 1998; Gaullier et al., 1998; Patki et al., 1998) were tested in the endosome fusion assay alone (Figure 2B) or in combination (data not shown). Of the five peptides, only the central region of the FYVE finger domain efficiently blocked fusion. Importantly, this effect is not simply due to an inhibition of PI(3)P-dependent EEA1 recruitment, since this peptide did not cause significant translocation of EEA1 from the endosome membrane to cytosol (data not shown). We therefore tested whether this peptide had any effect on the ability of EEA1 to bind syntaxin 13 in the biosensor assay. The interaction between EEA1 and syntaxin 13 was analyzed in the presence of increasing amounts of either the FYVE2 peptide, or as controls, the IQ domain and the FYVE1 peptide. As seen in Figure 2C, we found no alteration in the binding activity between EEA1 and syntaxin 13 in the presence of either the IQ domain or the FYVE1 peptide. However, in agreement with the dose-dependent block in endosome fusion (Figure 2C), equivalent concentrations of the FYVE2 peptide completely disrupted the interaction between EEA1 and syntaxin 13 in the biosensor assay. These two sets of experiments indicate that the inhibition of endosome fusion directly correlates with the obstruction of the EEA1/syntaxin 13 interaction.

EEA1 Forms Oligomeric Complexes Containing NSF and Rabaptin-5

We employed velocity sedimentation gradients in order to visualize the dynamic assembly of protein complexes

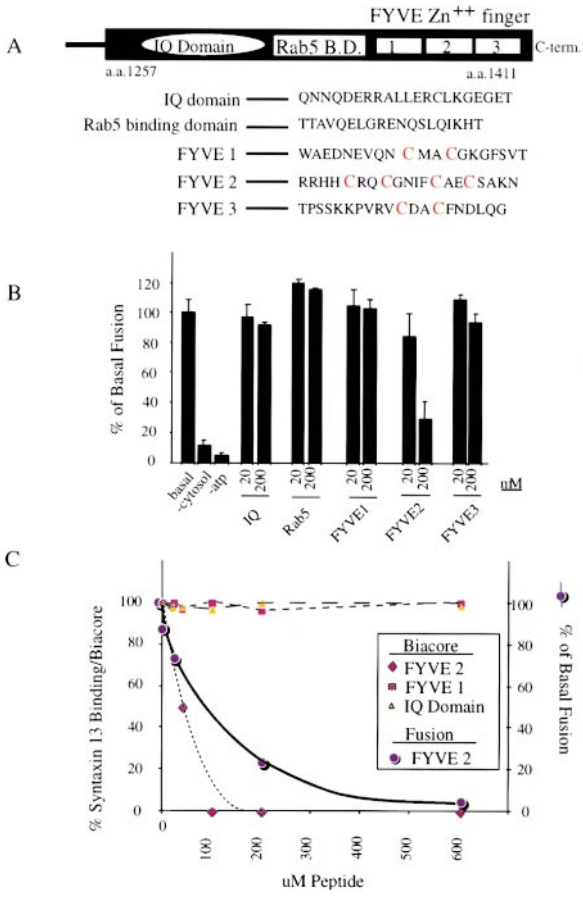

Figure 2. Synthetic Peptide Inhibits Fusion by Interfering with the EEA1/Syntaxin 13 Interaction

(A) The domain structure of EEA1(1257–1411) is indicated, including the IQ domain, potential Rab5-binding domain, and the FYVE Zn^{2+} finger. The sequences of each synthetic peptide are listed. Conserved cysteine residues within the FYVE finger are highlighted.

(B) Standard fusion assays (as in Figure 1) were performed containing increasing amounts of each synthetic peptide.

(C) EEA1(1257–1411)GST was immobilized on a carboxymethyldextran chip as in Figure 1. Synthetic peptides were first added to a final concentration of 20 μM, 40 μM, 100 μM, or 200 μM to obtain a stable signal prior to the addition of 20 μM recombinant syntaxin 13. The data are depicted as a percentage of syntaxin 13 binding to EEA1(1257–1411) in the absence of synthetic peptide. Background values (binding to immobilized GST) were subtracted from each signal obtained with EEA1(1257–1411)GST, as in Figure 1. Diamonds indicate values obtained with the FYVE2 peptide; squares, FYVE1; and triangles, the IQ domain. The titration of the FYVE2 peptide into the fusion assay (circles) is also shown using the secondary y axis.

formed on the membrane following Rab effector recruitment from cytosol. Most importantly, we examined the behavior of endogenous proteins to avoid nonphysiological interactions due to protein overexpression. We chose to utilize chemical cross-linkers for two reasons: (1) protein–protein interactions leading to regulated fusion are most likely transient in nature and could be arrested using a cross-linker, and (2) to stabilize interactions that may be otherwise disrupted by the addition of detergents to solubilize membranes. Standard fusion reactions were incubated for 25 min at 37°C in order to allow the recruitment of cytosolic effector proteins onto

the endosome membrane. Following this, the 20 Å, cleavable, cysteine-specific cross-linker 1,4-Di-[3′-(2′-pyridyldithio)-propionamido] butane (DPDPB) was added to the fusion reaction. This cross-linker was chosen over amine-specific and heterobifunctional cross-linkers, since a titration screen (of a panel of cross-linkers) demonstrated that DPDPB did not cause nonspecific aggregation while selectively linking Rab5 and RabGDI in cytosol (data not shown). Cross-linked membranes were solubilized, and the mixture was subjected to glycerol gradient centrifugation. Upon examination by Western blotting, cytosolic EEA1 migrated in fractions 4 and 5 and shifted to fractions 5 and 6 upon the addition of the cross-linker (Figure 3A). This small shift observed on cytosolic EEA1 is consistent with the reported dimerization (Callaghan et al., 1999). Furthermore, little or no change in the migration of cytosolic Rabaptin-5 and NSF (data not shown) was observed. Strikingly, upon addition of endosomes, a fraction of EEA1 underwent a major shift into a high molecular weight complex at the bottom of the gradient (lanes 17 and 18, Figure 3A, middle panel). Therefore, the appearance of this high molecular weight peak is specifically due to an interaction of EEA1 with the endosomal membrane.

In order to analyze sufficient protein complexes on the membrane, the fusion reaction was scaled up 25-fold. Following fusion and cross-linking, cytosolic proteins and potential aggregates were removed by reisolating the membranes through a sucrose floatation gradient. Following solubilization of the membranes, the sedimentation time through glycerol was reduced to 3 hr to increase the resolution of the high molecular weight complex. Under basal conditions, membrane-bound EEA1 was resolved into two broad pools (Figure 3B), the first pool migrating at the top of the gradient between 4.9S and 20S (fractions 2–5, Figure 3B) and a second pool migrating beyond the 65S marker. The same blots were probed against a number of antibodies to determine the overall pattern of known docking/fusion components (Rabaptin-5, NSF, α-SNAP, and syntaxin 13; see Figure 3B). α-SNAP and the t-SNAREs colocalized within the first five fractions, consistent with the function of α-SNAP as an NSF adaptor protein stably bound to SNAREs. However, most unexpectedly, the bulk of NSF did not colocalize with either syntaxin, or α-SNAP, but comigrated with Rab effectors within large oligomers extending beyond 65S (Figure 3B). This large pool completely overlapped with the pattern of EEA1, Rabaptin-5, and Rabex-5 (data not shown), suggesting a multifunctional complex of proteins on the membrane. It is important to note that the transferrin receptor and α-SNAP did not oligomerize with NSF and the Rab effector proteins, ruling out unspecific aggregation due to the cross-linking approach (Figure 3B). Rab5 was also not found in the large oligomers of EEA1, even though it is known to bind and recruit EEA1 to the membrane (Simonsen et al., 1998). A possible trivial explanation for this could be the lack of appropriate cysteine residues in Rab5 available to the cross-linker, even though cytosolic Rab5 could be linked to Rab GDI (data not shown). Only low amounts of the SNAREs were typically found in the high molecular weight fractions at steady state. These observations lead to the conclusion that the Rab5 effectors and NSF each form complexes beyond 65S specifically on the endosomal membrane. The size and migration pattern of these proteins suggested that they may directly interact to form oligomers.

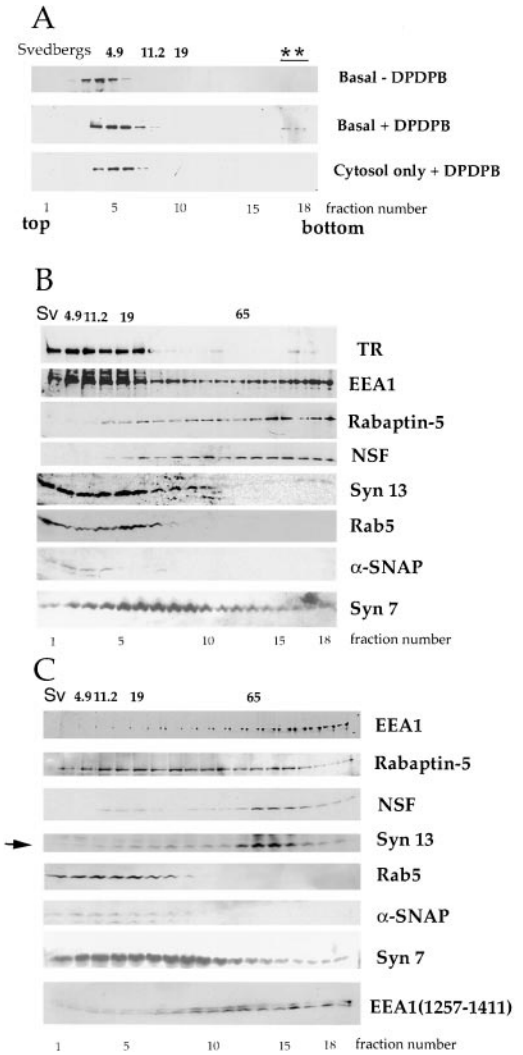

Figure 3. Membrane-Specific Oligomers Contain EEA1, Rabaptin-5, and NSF and, upon Synchronized Arrest, Syntaxin 13

(A) Two hundred microliter endosome fusion reactions (top and middle panel), or cytosol alone (bottom panel), were arrested by the addition of 5 mM cross-linking agent DPDPB (or mock treated, top panel) and solubilized. The total reaction was then subjected to a 25%–50% glycerol gradient for 16 hr centrifugation. Fractions were analyzed by Western blot for endogenous EEA1. Oligomeric EEA1 in fractions 17 and 18 are indicated by asterisks (middle panel).

(B) Five milliliter fusion reactions were incubated for 25 min at 37°C, following which, DPDPB was added, and endosomes were reisolated, solubilized, and loaded onto a 25%–50% glycerol gradient for 3 hr (see Experimental Procedures). Fractions were analyzed by Western blot as indicated. Basal refers to standard fusion assay conditions (Horiuchi et al., 1997). Size markers and fraction numbers are indicated.

(C) Recombinant EEA1(1257–1411)GST (3 μM) was added to a 5 ml basal fusion assay and the membranes processed exactly as in (B). Svedberg values and fraction numbers are indicated. Arrow highlights the shift of syntaxin 13 into the large oligomers.

EEA1(1257–1411)GST Sequesters Syntaxin 13 into the Large Oligomers

Basal fusion conditions do not allow a precise synchronization of the EEA1 docking and fusion process, and

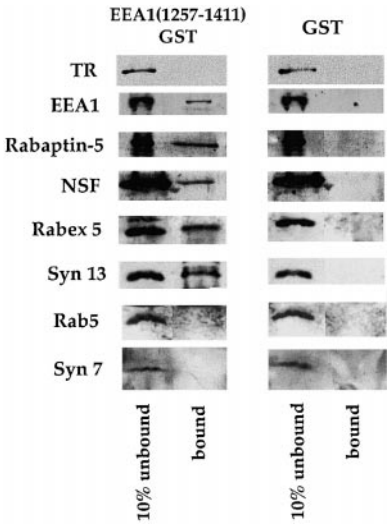

Figure 4. Glutathione S-Sepharose Retrieves a Complex of EEA1 (1257–1411)GST, NSF, Rabaptin-5, EEA1, and Syntaxin 13

Fusion assays (5 ml) containing 3 μM EEA1(1257–1411)GST or 3 μM GST were arrested with DPDPB as in Figure 3. The membranes were reisolated, solubilized, and incubated with glutathione S-Sepharose beads. Unbound proteins were washed extensively with standard fusion buffer (lacking DTT) containing 1% Triton X-100. Bound material was eluted in sample buffer, cleaving the cross-linker with 100 mM DTT. Ten percent of unbound material and the eluates were separated on SDS–PAGE and transferred to nitrocellulose for Western blots as indicated.

therefore, if the interaction of EEA1 and syntaxin 13 mediates a transition from docking to fusion, one would not expect to observe high levels of EEA1–syntaxin 13 complexes at steady state. However, the kinetically stable arrest in fusion induced by EEA1(1257–1411)GST (Figures 1A and 1D) allowed the analysis of molecular events taking place under a specific and synchronized block at the point of docking. EEA1(1257–1411)GST was added to the large scale fusion reaction at 3 μM, an amount sufficient to completely impair endosome fusion in vitro (Figure 1A). The recombinant protein was efficiently recruited to the membranes where it oligomerized together with endogenous EEA1, NSF, and Rabaptin-5 (Figure 3C, see below). The most remarkable effect was that EEA1(1257–1411)GST caused the majority of syntaxin 13 to shift specifically into the high molecular weight fractions without affecting the mobility of syntaxin 7, α-SNAP, or Rab5. This demonstrates that the behavior of syntaxin 13 is specific. Perhaps not suprisingly, truncated EEA1 also competed for the total recruitment of endogenous EEA1 to the endosome. Since 3 μM EEA1(1257–1411) cannot alone support docking in the absence of cytosol (S. Christoforidis and M. Z., unpublished data), the remaining levels of endogenous oligomeric EEA1 must be sufficient to mediate docking. The dramatic shift of syntaxin 13 into the large oligomers upon the addition of EEA1(1257–1411)GST suggested that a complex was stabilized between oligomeric NSF, Rabaptin-5, and EEA1 (both truncated and endogenous) with syntaxin 13. This possibility was directly tested by retrieving the complex through EEA1 (1257–1411)GST on glutathione S-Sepharose beads (Figure 4). The fusion reaction was carried out exactly as in Figure 3C in the presence of 3 μM EEA1(1257–1411)GST or GST alone. Endogenous EEA1, NSF, Rabaptin-5, Rabex-5, and syntaxin 13 were bound to EEA1(1257–1411)GST only in the presence of the cross-linker (data not shown) and were not retrieved in the presence of GST alone (Figure 4). These data demonstrate that there are direct complex interactions between EEA1, NSF, Rabaptin-5, Rabex-5, and syntaxin 13 that occur specifically on the membrane. Rab5, syntaxin 7, and the transferrin receptor were not part of this complex (Figure 4), consistent with the gradient analysis. These data suggest that recombinant EEA1(1257–1411)GST locks the oligomeric complex together in a docked, but fusion-incompetent conformation where the t-SNARE is unable to complete a fusion event.

Microdomains of Rab5 and Effectors Exist on the Surface of the Endosomes

The size of the EEA1 oligomers containing NSF and Rabaptin-5 in vitro suggested that this structure may be visible in vivo. However, the resolution of microscopic analysis is too low to detect such macromolecular interactions. To facilitate the morphological analysis, we induced their enlargement by the expression of Rab5Q79L and analyzed EEA1 on these structures. Confocal microscopic analysis of BHK cells expressing Rab5Q79L demonstrated the presence of endogenous EEA1 in clusters of higher intensity on the endosome surface (Figure 5A). Although the size of the clusters is most likely exaggerated due to the coalescence of several endosomes into enlarged vesicles, the appearance of EEA1 within microdomains is consistent with the biochemical observations of oligomeric complexes of EEA1 on the membrane. To ensure that the clustering is not due to antibody effects during fixation, we repeated the experiment using low levels of EEA1(1257–1411)GFP and higher amounts of Rab5Q79L to keep the endocytic structures enlarged. Clusters of the GFP construct were observed as with the endogenous staining and were seen to overlap with Rab5 (Figure 5B). Video analysis of these cells demonstrated that the patches also move laterally on the plane of the membrane over time (data not shown). Although the observation of fluorescent patches on the enlarged endosomes may not exactly equate to the biochemical oligomers seen using glycerol gradients, it is consistent with the idea that Rab5, through the recruitment of specific effector proteins, is involved in organizing microdomains containing the membrane docking and fusion machinery.

ATPγS and α-SNAP Dynamics Affect Oligomer Assembly

The observation that NSF participates within oligomers of EEA1 and Rabaptin-5 suggested that the complex dynamics could be regulated by the ATPase activity of NSF. To test this, we examined the profiles of these proteins on the glycerol gradients under conditions where the ATPase activity is either blocked (ATPγS) or stimulated (addition of α-SNAP + ATP). α-SNAP has been shown to stimulate the activity of NSF (Barnard et al., 1997). Whereas 0.5 μM α-SNAP slightly stimulated the fusion reaction, a 10-fold excess (5 μM) inhibited the reaction (Figure 6A). Fusion experiments were performed exactly as in Figure 3B in the presence of 1 mM

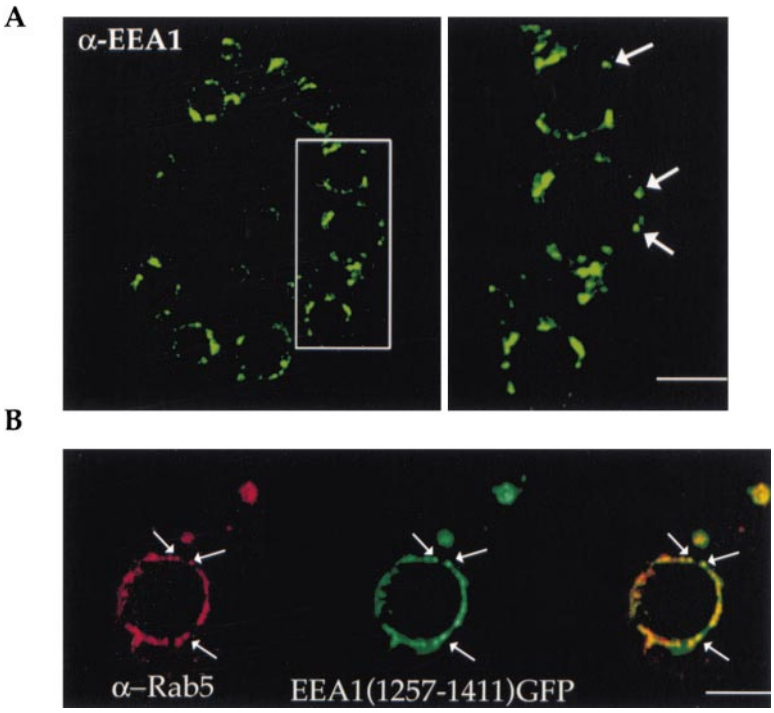

Figure 5. Rab5 and Its Effectors Form Microdomains on the Endosome In Vivo

(A) BHK cells infected with T7 vaccinia virus were transfected with mycRab5Q79L for 4 hr before fixation and staining endosomes with human EEA1 antibodies. A higher magnification of the endosomes is shown in the insert, which highlights (arrows) microdomains of EEA1 around the enlarged vesicles.

(B) BHK cells were vaccinia infected and transfected with both mycRab5Q79L and EEA1(1257–1411)GFP for 4 hr before fixation, and GFP signal was compared with antibody staining obtained with polyclonal anti-Rab5. Arrows highlight colocalization within microdomains; bar, 5 μm.

ATPγS or 5 μM α-SNAP, and the purified membranes were subjected to gradient analysis. ATPγS and α-SNAP had opposite effects on the oligomeric complex. In the presence of ATPγS, the high molecular weight oligomeric pool of EEA1 was stabilized, along with Rabaptin-5, NSF (Figure 6B, top panel), and Rabex-5 (data not shown). The low molecular weight pool of EEA1 observed under basal conditions was severely diminished (compare EEA1 fractions 2–5, Figure 3B with Figure 6B). Syntaxin 13 exhibited a slight shift above 20S, consistent with earlier observations (Hohl et al., 1998). Most dramatic, however, was the pattern obtained upon addition of 5 μM α-SNAP, where the high molecular weight oligomer disassembled (compare EEA1 in top and bottom panels, Figure 6B). Under these conditions, EEA1 shifted into the lower pool and Rabaptin-5 migrated toward the 30S position, a distinct position from EEA1. NSF remained oligomeric, although a substantial pool also shifted to the middle of the gradient. Under each condition, Rab5 and the transferrin receptor remained unaltered (data not shown). When the experiment was performed with an equivalent concentration of mutant α-SNAP(L294A), which blocks the ATPase activity of NSF (Barnard et al., 1997), the pattern of EEA1 was similar to that with ATPγS (data not shown), further suggesting a requirement for ATP hydrolysis by NSF to disassemble the complex. These results clearly demonstrate the specificity of the cross-linking where a dynamic pattern of protein complexes can be specifically resolved through the gradient. More importantly, these data demonstrate the integration of the Rab5 effector proteins within the ATPase cycle of NSF.

Discussion

In this study we report a novel property of the Rab5 effector proteins, namely their ability to oligomerize with components of the SNARE machinery. The docking protein EEA1, which typically exists as a homodimer in cytosol, upon recruitment to the endosome membrane assembles into macromolecular complexes with Rabaptin-5, Rabex-5, and NSF. We further demonstrate that the t-SNARE syntaxin 13 functions specifically in early endosome fusion. Syntaxin 13 dynamically partitions into the oligomeric complex as a result of a direct interaction with EEA1, and this interaction is essential for early endosome fusion. First, recombinant syntaxin 13 specifically binds EEA1 in vitro. Second, a C-terminal fragment of EEA1 interferes with the endogenous EEA1/syntaxin 13 interaction, induces the stable incorporation of syntaxin 13 into the oligomers, and arrests membrane fusion. Third, a synthetic peptide from the central region of the FYVE finger domain blocks the interaction between EEA1 and syntaxin 13 and impairs endosome fusion. Further analysis of the oligomeric complex between NSF, Rabaptin-5, and EEA1 reveals an unexpected role for the ATPase activity of NSF in regulating oligomerization of the Rab effectors and the transition from membrane docking to fusion.

Based on these and previous results, we propose the following model combining the function of the Rab and SNARE machineries in endosome membrane docking and fusion (Figure 7). Rab5:GTP, activated by the Rabaptin-5/Rabex-5 complex (Horiuchi et al., 1997), recruits EEA1 on the membrane where local pools of PI(3)P stably anchor EEA1 (Patki et al., 1997; Mills et al., 1998; Simonsen et al., 1998) and facilitate oligomerization by the lateral assembly of EEA1 units into the NSF/EEA1/Rabaptin-5/Rabex-5 complex. This leads ultimately to the formation of membrane microdomains, which function as tethering platforms for incoming vesicles by virtue of EEA1 (Christoforidis et al., 1999). Rabaptin-5/Rabex-5 may ensure sufficient levels of activated Rab5 to recruit EEA1 and maintain the dynamic equilibrium

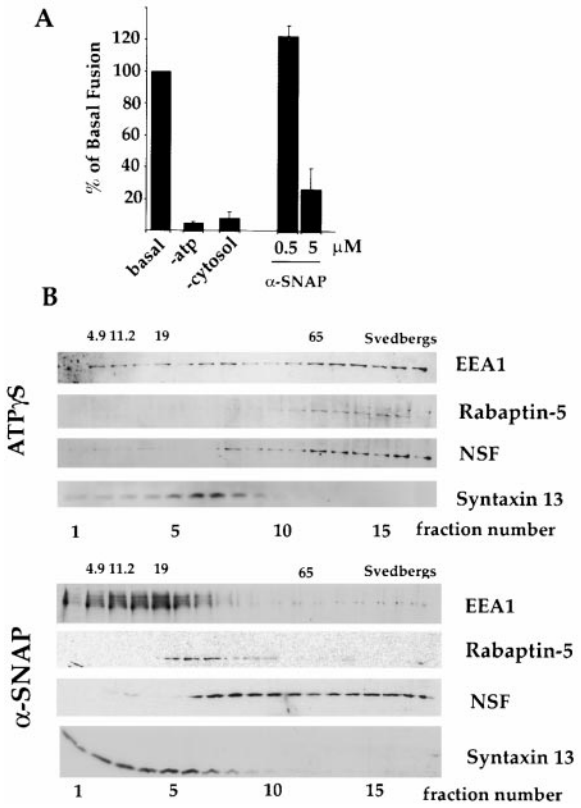

Figure 6. Dynamic ATPase Activity of NSF Affects the Assembly and Disassembly of the Oligomeric Complex

(A) Standard fusion assays were performed as in Figure 1, with the addition of increasing micromolar amounts of α-SNAP. Controls are indicated.

(B) Fusion reactions (5 ml) were performed exactly as in Figure 3B, with the addition of 1 mM ATPγS in the absence of an ATP regenerating system (top panel), or 5 μM α-SNAP (bottom panel). Fusion reactions were cross-linked, and membranes were reisolated, solubilized, and separated on 25%–50% glycerol for 3 hr as in Figure 3B and analyzed by Western blot. Size markers and fraction numbers are indicated.

between assembly and disassembly of the oligomeric structures. However, Rab5 itself may not remain stably bound to these molecules but rather undergo multiple GTPase cycles (Rybin et al., 1996) to recruit a multiplicity of effectors (Christoforidis et al., 1999). A consequence of the dynamic recruitment and assembly of Rab effectors into these oligomeric complexes is the fact that the microdomains appear heterogeneous in size rather than a stable and defined protein complex such as the exocyst (Guo et al., 1999). The unique features of these microdomains (i.e., size, biochemical composition, localization, and functional properties) suggest that Rab5 and its effectors may play a central role not only in the regulation of membrane trafficking to early endosomes but also in the biogenesis of this organelle. Importantly, no oligomerization of EEA1, Rabaptin-5/Rabex-5, or NSF was detected in cytosol, despite the abundance of these proteins. It is likely that the recruitment of these proteins to the membrane increases their local concentration, thus allowing for oligomerization. In addition, oligomerization on the membrane may increase the affinities of the interactions compared with those between individual proteins. The oligomers, which exist at steady state under basal conditions, are then able to transiently incorporate syntaxin 13 in order to drive fusion (see below). An increased affinity for interactions within the context of an oligomer may explain why the IC50 (~1.5 μM, Figure 1A) for the inhibitory effect of EEA1(1257–1411)GST in the endosome fusion reaction (where it oligomerizes) is lower than the estimated affinity for syntaxin 13 from biosensor analysis (18 μM, Figure 1). We cannot exclude the possibility that EEA1(1257–1411) GST may also exert its inhibitory effect through interactions with other proteins of the oligomers. However, the concentrations required for the FYVE2 peptide to block endosome fusion are entirely consistent with a disruption of the EEA1–syntaxin 13 interaction as determined by the biosensor analysis. Although expected to compete for v-t SNARE pairing, recombinant syntaxin 13 may also impair the binding of EEA1 to endogenous syntaxin 13, since it blocks fusion at concentrations similar to the K_D of this interaction (Figure 1A).

A surprising finding of our study is the presence and activity of NSF in the EEA1 oligomers. We envision two important mechanistic implications. First, the ATPase activity of NSF modulates the dynamics of the oligomers, since EEA1 and Rabaptin-5 are either stabilized (ATPγS) or released (α-SNAP) from the NSF oligomers upon modulation of the ATP cycle (Figure 6B). ATP hydrolysis by NSF requires the full length of EEA1 to disassemble the oligomer, since the intercalation of the C-terminal fragment of EEA1 shifts the remaining endogenous protein into large fusion-incompetent oligomers (Figure 3C). The inhibitory effect of both ATPγS and excess α-SNAP in endosome fusion strongly suggests a functional requirement for dynamic oligomeric complexes. In relation to our observations, the AMPA receptor GluR2 bound reversibly to NSF, its release dependent upon ATP hydrolysis (Nishimune et al., 1998; Osten et al., 1998; Song et al., 1998). Therefore, NSF has been proposed to act as a chaperone modulating the clustering of AMPA receptors with the GRIP molecular scaffold (Lin and Sheng, 1998). Our results also suggest that NSF can function as a chaperone to regulate the assembly of Rab effector protein complexes on the endosome. Second, the activity of NSF within the oligomers strongly suggests that EEA1 may contribute a novel regulatory function to temporally couple vesicle docking with SNARE priming. Given the established function of NSF in priming SNAREs (Rothman, 1994; Hay and Scheller, 1997), we propose that EEA1-mediated membrane tethering would trigger oligomeric NSF to prime SNAREs locally. Previously, there have been examples of proteins proposed to modulate SNARE priming by a different mechanism (i.e., by relieving the negative regulation imposed by Vps45p/n-Sec1p/MUNC-18) (Burd et al., 1997; Lupashin and Waters, 1997; Fujita et al., 1998). This list of proteins includes Vac1p, another Rab effector protein containing a FYVE Zn^{2+} finger (Peterson et al., 1999). Once SNAREs have become primed by NSF, they must remain primed long enough for trans-pairing to occur. In vacuolar fusion, LMA1 is transferred from NSF to the t-SNARE (Vam3p) upon ATP hydrolysis, where it is thought to maintain primed t-SNAREs until fusion is complete (Xu et al., 1998). Similarly, the release of Rab effectors upon ATP hydrolysis (Figure 6B, bottom panel)

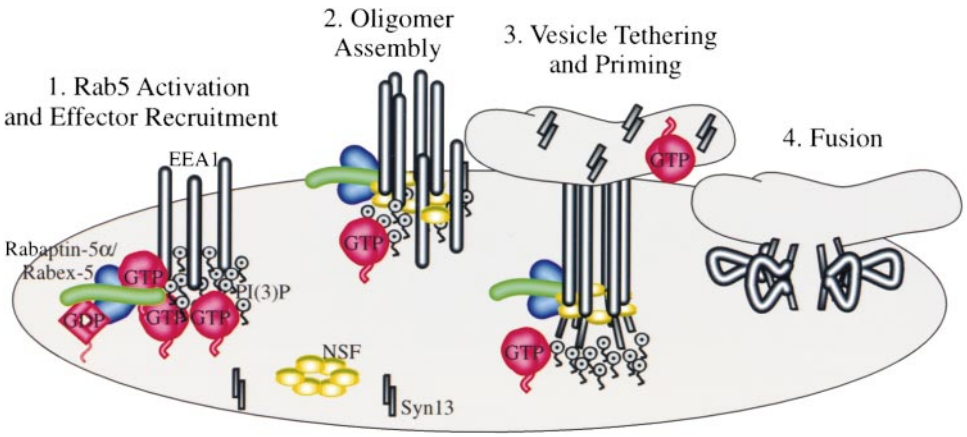

Figure 7. Model of Events Leading to Endosome Fusion

(1) Rab5 activation and effector recruitment. Rab5:GDP is delivered to the membrane where Rabex-5 mediates nucleotide exchange. Rabaptin-5 (complexed to Rabex-5) stabilizes Rab:GTP, which can subsequently recruit EEA1.

(2) EEA1 oligomer assembly. EEA1 requires PI(3)P for stable membrane recruitment, which may participate in the assembly of oligomers containing NSF, Rabaptin-5, and Rabex-5.

(3) Docking and priming. EEA1 mediates vesicle docking, which can be directly coupled to SNARE priming since NSF is incorporated within the docking complex.

(4) EEA1–syntaxin 13 interaction for fusion. Docking is intimately linked to fusion, since EEA1 transiently incorporates syntaxin 13 into the large oligomers perhaps to form a fusion pore reminiscent of viral fusion pores (see text for details).

may trigger the interaction between EEA1 and syntaxin 13. Clearly, there is much to be learned about the dynamics of these interactions, but it is evident that ATP hydrolysis by NSF not only results in the priming of SNAREs, but also controls the coupling of Rab effectors with the NSF oligomers.

Finally, the requirement for large, oligomeric complexes in vesicle fusion is remarkably similar to the formation of a fusion pore by viral glycoproteins. For example, fusion proteins of both influenza hemagglutinin (HA) and HIV (gp120/gp41) undergo a conformational change triggered by low pH (HA) or interactions with host receptors (gp120/gp41). This structural change exposes domains thought to mediate the formation of an oligomeric pore responsible for fusion (Doms and Helenius, 1986; Bentz et al., 1990; Stegmann et al., 1990; Danieli et al., 1996). Consistent with this, it was recently demonstrated that the baculovirus fusion protein gp64 transiently forms large oligomers (over 2 MDa) at the point of viral contact with the cell (Markovic et al., 1998). Much in the same way as viral fusion proteins form oligomeric complexes, oligomeric EEA1 could physically cooperate with syntaxin 13 to form a fusion pore (see model, Figure 7). We speculate that, following membrane tethering, EEA1 may undergo a structural change triggered by the hydrolysis of ATP by NSF, or perhaps a calcium-dependent switch through the IQ domain. In this way, the combination of EEA1 and SNAREs would be functionally equivalent to the highly efficient viral fusion proteins (Figure 7). The requirement for a Rab effector in pore formation would explain the low efficiency of fusion observed in a purified system containing only SNARE proteins (Weber et al., 1998). Furthermore, the transient nature of a fusion pore would explain why only trace amounts of syntaxin 13 are observed with oligomeric EEA1 at steady state when few endosomes are predicted to be engaged in docking and fusion at a given time (Figure 3B). The core function of EEA1 as an endosome docking protein (Christoforidis et al., 1999), combined with the transient nature of the interaction with syntaxin 13, now provides evidence of a temporal and dynamic link between Rab5-regulated docking and SNARE-dependent fusion. The implications of these interactions in the context of a fusion pore provide important novel directions for future studies in vesicular transport.

Experimental Procedures

Glycerol Gradient Analysis

For large scale experiments, 5 ml standard fusion reactions containing 800 μg purified endosomes from sHeLa cells and 25 mg HeLa cytosol with an energy regenerating system were incubated at 37°C for 25 min. The cysteine-specific cross-linker 1,4-Di-[3′-(2′-pyridyldithio)-propionamido] butane (DPDPB) (Pierce) was adjusted to 5 mM in DMSO (or DMSO alone) and further incubated for 30 min at 30°C. The cross-linker was quenched by the addition of 50 mM L-cysteine for 45 min at 4°C. Membranes were isolated from the reaction by centrifugation at 275,000 × g (80,000 rpm in TLA100.4 rotor) for 30 min onto a 65% sucrose cushion. The membranes were resuspended, adjusted to 40.6% sucrose w/v, and overlayed with a 35%/25% sucrose (+3 mM imidazole [pH 7.4]) step gradient. Membranes were collected from the 35%/25% interface after centrifugation at 214,000 × g (50,000 rpm in TLS55 rotor) for 1 hr at 4°C and concentrated by a further centrifugation at 275,000 × g (80,000 rpm in TLA100.4) for 30 min before adjusting the final volume to 200 μl in modified fusion buffer lacking DTT (12.5 mM HEPES, 1.5 mM magnesium acetate, 75 mM potassium acetate [pH 7.4] with 2% Triton X-100). To ensure complete solubilization of the membranes, the sample was sonicated in a bath sonicator for three 10 s pulses at 20°C, followed by a 30 min incubation at 4°C. Solubilized material was loaded onto the top of a 12-step 25%–50% glycerol gradient prepared in fusion buffer (as above) with 2% Triton X-100 and centrifuged for 3 hr at 214,000 × g (50,000 rpm in TLS55). In each experiment, size markers were resolved through a separate gradient (transferrin = 4.9S, catalase = 11.2S, thyroglobulin = 19S, and ferritin = 65S). Eighteen fractions of 110 μl were collected from the top of the gradients to the bottom, and 80 μl was taken for loading onto

an 8%–17% gradient SDS–PAGE. Prior to gel loading, the cross-linker was cleaved by the addition of 100 mM fresh DTT. Proteins were transferred to nitro-cellulose and analyzed by Western blotting.

Antibodies and Recombinant Proteins

The human cDNAs encoding syntaxin 13 and syntaxin 7 were purchased from Genome Systems and confirmed by sequencing. Syntaxins 7ΔC and 13ΔC were cloned into pGEX-5X and pGEX-4T (Pharmacia), respectively, and expressed in DH5α bacteria for biosensor experiments and antibody generation. cDNA encoding pQEhis-NSF and pQEhis-α-SNAP were the kind gift of James Rothman and were used to produce recombinant proteins for polyclonal antibody preparation. Polyclonal Rab5 (46-4) and Rabaptin-5 (L146) have been characterized before (Stenmark et al., 1995). Anti-transferrin receptor monoclonal antibodies (H68.4) were purchased from Zymed (San Francisco, CA). Human antiserum against EEA1 was obtained from Ban-Hock Toh (Monash Medical School, Australia). Proteins and antibodies against Syntaxins 1, 2, 3, and 4 were the gift of Beatriz Quinones and Mark Bennett (University of California, Berkley, CA). Syntaxin 6 antibodies and proteins were supplied by Robert Piper (University of Oregon, Eugene, OR). cDNA encoding EEA1(1257–1411)GFP (from Harald Stenmark, Norwegian Radium Hospital, Norway) was subcloned into pGEX-5X3 for protein expression in DH5α bacteria. Cleavage of GST from the recombinant proteins was performed as per manufacturer's instructions.

Biosensor Assay

EEA1(1257–1411)GST or GST alone was coupled to carboxymethyl-dextran (CMD) coated biosensor cuvettes (Affinity, Germany) following the manufacturer's instructions. Protein interactions were monitored on IAsys Auto+Biosensor (Affinity) in binding buffer (20 mM HEPES [pH 7.4], 150 mM NaCl, 1 mM DTT). Regeneration of the sensor cuvette was achieved as described (Gournier et al., 1998). The observed binding curves were fit assuming single-phase kinetics, and single-phase association rates were accordingly calculated from the fits using the FastFit software (Affinity, Germany). Linear plots of the association rates versus ligand concentrations were fit to the data with a correlation coefficient of 0.96 and yield K_{on} and K_{off} values.

Immunofluorescence and Time-Lapse Microscopy

PGEM vectors containing cDNA for Rab5Q79L or EEA1(1257–1411)GFP were transfected into BHK cells 30 min after infection with attenuated vaccinia virus containing T7 RNA polymerase. After 4 hr transfection, cells were fixed and solubilized with 3% PFA and 0.1% Triton X-100 and stained with antibodies and analyzed on a confocal Leica TCS inverted microscope. Alternatively, for video microscopy analysis, cells transfected with Rab5Q79L and EEA1(1257–1411)GFP were expressed for 2 hr after which cyclohexamide was added for another hour. Video microscopy was carried out using the Zeiss Axiovert 10 inverted microscope equipped with a cooled slow-scan CCD (charge-coupled device) camara (Photometrics CH250) connected to a SUN workstation (Murphy et al., 1996).

Other

Endosome purification and the in vitro fusion assay were performed as described previously, and all fusion reactions were carried out for 25 min (Horiuchi et al., 1997). Synthetic peptides were supplied by Genosys Biotech (London) and solubilized in water to 2 mM.

Acknowledgments

Harald Stenmark has graciously provided the EEA1(1257–1411)GFP construct. Special thanks to S. Christoforidis and B. Sönnichsen for many great ideas and discussions. Thanks also to K. Simons, M. Kiebler, B. Hoflack, and members of the laboratory for critical reading of the manuscript. Graphic assistance was kindly provided by R. Turner. H. M. M. is the recipient of a Canadian MRC fellowship. This work was supported by the Max Planck Gesellschaft and grants from the Human Frontier Science Program (RG-432/96), European Union Training and Mobility of Researchers (ERB-CT96-0020), and Biomed (BMH4-97-2410) (M. Z.).

Received January 11, 1999; revised July 1, 1999.

References

Advani, R.J., Bae, H.R., Bock, J.B., Chao, D.S., Doung, Y.C., Prekeris, R., Yoo, J.S., and Scheller, R.H. (1998). Seven novel mammalian SNARE proteins localize to distinct membrane compartments. J. Biol. Chem. *273*, 10317–10324.

Barnard, R.J.O., Morgan, A., and Burgoyne, R.D. (1997). Stimulation of NSF ATPase activity by α-SNAP is required for SNARE complex disassembly and exocytosis. J. Cell Biol. *139*, 875–883.

Bean, A.J., and Scheller, R.H. (1997). Better late than never: a role for rabs late in exocytosis. Neuron *19*, 751–754.

Bennett, M.K., Garcia-Arraras, J.E., Elferink, L.A., Peterson, K., Fleming, A.M., Hazuka, C.D., and Scheller, R.H. (1993). The syntaxin family of vesicular transport receptors. Cell *74*, 863–873.

Bentz, J., Ellens, H., and Alford, D. (1990). An architecture for the fusion site of influenza hemagglutinin. FEBS Lett. *276*, 1–5.

Bock, J.B., Klumperman, J., Davanger, S., and Scheller, R. (1997). Syntaxin 6 functions in trans-Golgi network vesicle trafficking. Mol. Biol. Cell *8*, 1261–1271.

Burd, C.G., and Emr, S.D. (1998). Phosphatidylinositol(3)-phosphate signaling mediated by specific binding to RING FYVE domains. Mol. Cell *2*, 157–162.

Burd, C.G., Peterson, M., Cowles, C.R., and Emr, S.D. (1997). A novel Sec18p/NSF-dependent complex required for Golgi-to-endosome transport in yeast. Mol. Biol. Cell *8*, 1089–1104.

Calakos, N., Bennett, M.K., Peterson, K.E., and Scheller, R.H. (1994). Protein-protein interactions contributing to the specificity of intracellular vesicular trafficking. Science *263*, 1146–1149.

Callaghan, J., Simonsen, A., Gaullier, J.-M., Toh, B.-H., and Stenmark, H. (1999). The endosome fusion regulator early-endosome autoantigen 1 (EEA1) is a dimer. Biochem. J. *338*, 539–543.

Cao, X., Ballew, N., and Barlowe, C. (1998). Initial docking of ER-derived vesicles requires Uso1p and Ypt1p but is independent of SNARE proteins. EMBO J. *17*, 2156–2165.

Chao, D.S., Hay, J.C., Winnick, S., Prekeris, R., Klumperman, J., and Scheller, R.H. (1999). SNARE mediated trafficking dynamics in vivo. J. Cell Biol. *144*, 869–881.

Christoforidis, S., McBride, H.M., Burgoyne, R.D., and Zerial, M. (1999). The Rab5 effector EEA1 is a core component of endosome docking and fusion. Nature *397*, 621–625.

Coorssen, J.R., Blank, P.S., Tahara, M., and Zimmerberg, J. (1998). Biochemical and functional studies of cortical vesicle fusion: the SNARE complex and Ca^{2+} sensitivity. J. Cell Biol. *143*, 1845–1857.

Danieli, T., Pelletier, S.L., Henis, Y.I., and White, J.M. (1996). Membrane fusion mediated by the influenza virus hemagluttinin requires the concerted action of at least three hemagglutinin trimers. J. Cell Biol. *133*, 559–569.

Doms, R.W., and Helenius, A. (1986). Quaternary structure of influenza virus hemagglutinin after acid treatment. J. Virol. *60*, 833–839.

Finger, F.P., Hughes, T.E., and Novick, P. (1998). Sec3p is a spatial landmark for polarized secretion in budding yeast. Cell *92*, 559–571.

Fujita, Y., Shirataki, H., Sakisaka, T., Asakura, T., Ohya, T., Kotani, H., Yokoyama, S., Nishioka, H., Matsuura, Y., Mizoguchi, A., et al. (1998). Tomosyn: a syntaxin-1-binding protein that forms a novel complex in the neurotransmitter release process. Neuron *20*, 905–915.

Gaullier, J.-M., Simonsen, A., D'Arrigo, A., Bremnes, B., Stenmark, H., and Aasland, R. (1998). FYVE fingers bind PtdIns(3)P. Nature *394*, 432–433.

Gonzalez, L.J., and Scheller, R.H. (1999). Regulation of membrane trafficking: structural insights from a Rab/effector complex. Cell *96*, 755–758.

Gournier, H., Stenmark, H., Rybin, V., Lippe, R., and Zerial, M. (1998).

Two distinct effectors of the small GTPase Rab5 cooperate in endocytic membrane fusion. EMBO J. *17*, 1930–1940.

Guo, W., Roth, D., Walch-Solimena, and Novick, P. (1999). The exocyst is an effector for Sec4p, targeting secretory vesicle to sites of exocytosis. EMBO J. *18*, 1071–1080.

Hanson, P.I., Roth, R., Morisaki, H., Jahn, R., and Heuser, J.E. (1997). Structure and conformational changes in NSF and its membrane receptor complexes visualized by quick-freeze/deep-etch electron microscopy. Cell *90*, 523–535.

Hay, J.C., and Scheller, R.H. (1997). SNAREs and NSF in targeted membrane fusion. Curr. Opin. Cell Biol. *9*, 505–512.

Hay, J.C., Klumperman, J., Oorschot, V., Steegmaier, M., Kuo, C.S., and Scheller, R.H. (1998). Localization, dynamics, and protein interactions reveal distinct roles for ER and Golgi SNAREs. J. Cell Biol. *141*, 1489–1502.

Hohl, T.M., Parlati, F., Wimmer, C., Rothman, J.E., Sollner, T.H., and Engelhardt, H. (1998). Arrangement of subunits in 20S particles consisting of NSF, SNAPs, and SNARE complexes. Mol. Cell *2*, 539–548.

Holthuis, J.C., Nichols, B.J., Dhruvakumar, S., and Pelham, H.R. (1998). Two syntaxin homologues in the TGN/endosomal system of yeast. EMBO J. *17*, 113–126.

Horiuchi, H., Lippé, R., McBride, H.M., Rubino, M., Woodman, P., Stenmark, H., Rybin, V., Wilm, M., Ashman, K., Mann, M., and Zerial, M. (1997). A novel Rab5 GDP/GTP exchange factor complexed to Rabaptin-5 links nucleotide exchange to effector recruitment and function. Cell *90*, 1149–1159.

Klumperman, J., Kuliawat, R., Griffith, J.M., Geuze, H.J., and Arvan, P. (1998). Mannose-6-phosphate receptors are sorted from immature secretory granules via adaptor protein AP-1, clathrin, and syntaxin 6-positive vesicles. J. Cell. Biol. *141*, 359–371.

Lian, J.P., Stone, S., Jiang, Y., Lyons, P., and Ferro-Novick, S. (1994). Ypt1p implicated in v-SNARE activation. Nature *372*, 698–701.

Lin, J.W., and Sheng, M. (1998). NSF and AMPA receptors get physical. Neuron *21*, 267–270.

Lupashin, V.V., and Waters, M.G. (1997). t-SNARE activation through transient interaction with a rab-like guanosine triphosphatase. Science *276*, 1255–1258.

Markovic, I., Pulyaeva, H., Sokoloff, A., and Chernomordik, L.V. (1998). Membrane fusion mediated by baculovirus gp64 involves assembly of stable gp64 trimers into multiprotein aggregates. J. Cell Biol. *143*, 1155–1166.

Mills, I.G., Jones, A.T., and Clague, M.J. (1998). Involvement of the endosomal autoantigen EEA1 in homotypic fusion of early endosomes. Curr. Biol. *8*, 881–884.

Mu, F., Callaghan, J.M., Steele-Mortimer, O., Stenmark, H., Parton, R.G., Campbell, P.L., McCluskey, J., Yeo, J.P., Tock, E.P.C., and Toh, B.H. (1995). EEA1, an early endosome-associated protein. J. Biol. Chem. *270*, 13503–13511.

Murphy, C., Saffrich, R., Grummt, M., Gournier, H., Rybin, V., Rubino, M., Auvinen, P., Lutke, A., Parton, R.G., and Zerial, M. (1996). Endosome dynamics regulated by a Rho protein. Nature *384*, 427–432.

Nakamura, N., Lowe, M., Levine, T.P., Rabouille, C., and Warren, G. (1997). The vesicle docking protein p115 binds GM130, a cis-Golgi matrix protein, in a mitotically regulated manner. Cell *89*, 445–455.

Nishimune, A., Isaac, J.T.R., Molnar, E., Noel, J., Nash, S.R., Tagaya, M., Collingridge, G.L., Nakanishi, S., and Henley, J.M. (1998). NSF binding to GluR2 regulates synaptic transmission. Neuron *21*, 87–97.

Novick, P., and Zerial, M. (1997). The diversity of Rab proteins in vesicle transport. Curr. Opin. Cell Biol. *9*, 496–504.

Osten, P., Srivastava, S., Inman, G.J., Vilim, F.S., Khatri, L., Lee, L.M., States, B.A., Einheber, S., Milner, T.A., Hanson, P.I., and Ziff, E.B. (1998). The AMPA receptor GluR2 C terminus can mediate a reversible, ATP-dependent interaction with NSF and α- and β-SNAPs. Neuron *21*, 99–110.

Patki, V., Virbasius, J., Lane, W.S., Toh, B.H., Shpetner, H.S., and Corvera, S. (1997). Identification of an early endosomal protein regulated by phosphatidylinositol 3-kinase. Proc. Natl. Acad. Sci. USA *94*, 7326–7330.

Patki, V., Lawe, D.C., Corvera, S., Virbasius, J.V., and Chawla, A. (1998). A functional PtdIns(3)P-binding motif. Nature *394*, 433–434.

Peters, C., and Mayer, A. (1998). Ca^{2+}/calmodulin signals the completion of docking and triggers a late step of vacuole fusion. Nature *396*, 575–580.

Peterson, M.R., Burd, C.G., and Emr, S.D. (1999). Vac1p coordinates Rab and phosphatidylinositol 3-kinase signaling in Vps45p-dependent vesicle docking/fusion at the endosome. Curr. Biol. *9*, 159–162.

Pfeffer, S.R. (1999). Transport vesicle targeting: tethers before SNAREs. Nat. Cell Biol. *1*, E17–E22.

Poirier, M.A., Xiao, W., Macosko, J.C., Chan, C., Shin, Y.K., and Bennett, M.K. (1998). The synaptic SNARE complex is a parallel four-stranded helical bundle. Nat. Struct. Biol. *5*, 765–769.

Prekeris, R., Klumperman, J., Chen, Y.A., and Scheller, R.H. (1998). Syntaxin 13 mediates cycling of plasma membrane proteins via tubulovesicular recycling endosomes. J. Cell Biol. *143*, 957–971.

Rothman, J.E. (1994). Mechanisms of intracellular protein transport. Nature *372*, 55–63.

Rybin, V., Ullrich, O., Rubino, M., Alexandrov, K., Simon, I., Seabra, M.C., Goody, R., and Zerial, M. (1996). GTPase activity of rab5 acts as a timer for endocytic membrane fusion. Nature *383*, 266–269.

Schimmoller, F., Simon, I., and Pfeffer, S.R. (1998). Rab GTPases, directors of vesicle docking. J. Biol. Chem. *273*, 22161–22164.

Simonsen, A., Lippé, R., Christoforidis, S., Gaullier, J.-M., Brech, A., Callaghan, J., Toh, B.-H., Murphy, C., Zerial, M., and Stenmark, H. (1998). EEA1 links phosphatidylinositol 3-kinase function to Rab5 regulation of endosome fusion. Nature *394*, 494–498.

Søgaard, M., Tani, K., Ruby Ye, R., Geromanos, S., Tempst, P., Kirchhausen, T., Rothman, J.E., and Söllner, T. (1994). A Rab protein is required for the assembly of SNARE complexes in the docking of transport vesicles. Cell *78*, 937–948.

Song, I., Kamboj, S., Xia, J., Dong, H., Liao, D., and Huganir, R.L. (1998). Interaction of the N-ethylmaeimide-sensitive factor with AMPA receptors. Neuron *21*, 393–400.

Stegmann, T., White, J.M., and Helenius, A. (1990). Intermediates in influenza induced membrane fusion. EMBO J. *9*, 4231–4241.

Stenmark, H., Vitale, G., Ullrich, O., and Zerial, M. (1995). Rabaptin-5 is a direct effector of the small GTPase Rab5 in endocytic membrane fusion. Cell *83*, 423–432.

Sutton, R.B., Fasshauer, D., Jahn, R., and Brunger, A.T. (1998). Crystal structure of a SNARE complex involved in synaptic exocytosis at 2.4 Å resolution. Nature *395*, 347–353.

Tang, B.L., Tan, A.E.H., Lim, L.K., Lee, S.S., Low, D.Y.H., and Hong, W. (1998). Syntaxin 12, a member of the syntaxin family localized to the endosome. J. Biol. Chem. *273*, 6944–6950.

Ungermann, C., Sato, K., and Wickner, W. (1998). Defining the functions of trans-SNARE pairs. Nature *396*, 543–548.

VanRheenen, S.M., Cao, X., Lupashin, V.V., Barlowe, C., and Waters, G.M. (1998). Sec35p, a novel peripheral membrane protein, is required for ER to Golgi vesicle docking. J. Cell Biol. *141*, 1107–1119.

von Mollard, G.F., Nothwehr, S.F., and Stevens, T.H. (1997). The yeast v-SNARE Vti1p mediates two vesicle transport pathways through interactions with the t-SNAREs Sed5p and Pep12p. J. Cell Biol. *137*, 1511–1524.

Weber, T., Zemelman, B.V., McNew, J.A., Westermann, B., Gmachl, M., Parlati, F., Solner, T., and Rothman, J.E. (1998). SNAREpins: minimal machinery for membrane fusion. Cell *92*, 759–772.

Wong, S.H., Xu, Y., Zhang, T., and Hong, W. (1998). Syntaxin 7, a novel syntaxin member associated with the early endosomal compartment. J. Biol. Chem. *273*, 375–380.

Xu, Z., Sato, K., and Wickner, W. (1998). LMA1 binds to vacuoles at Sec18p (NSF), transfers upon ATP hydrolysis to a t-SNARE (Vam3p) complex, and is released during fusion. Cell *93*, 1125–1134.

Yang, B., Gonzalez, L.J., Prekeris, R., Steegmaier, M., Advani, R.J., and Scheller, R.H. (1999). SNARE interactions are not selective. Implications for membrane fusion specificity. J. Biol. Chem. *274*, 5649–5653.